NANO LETTERS

2003
Vol. 3, No. 2
207−211

Novel Approach to the Fabrication of Macroporous Polymers and Their Use as a Template for Crystalline Titania Nanorings

Dong Kee Yi and Dong-Yu Kim*

Center for Frontier Materials, Department of Materials Science and Engineering, Kwang-Ju Institute of Science and Technology, Oryong-dong 1, Puk-gu, Kwang-Ju 500-712, Republic of Korea

Received October 4, 2002; Revised Manuscript Received November 25, 2002

ABSTRACT

This paper presents a novel method for fabricating two- and three-dimensional (2D/3D) polymer macroporous structures and demonstrates their use as templates for the production of crystalline titania nanorings. 2D honeycomb and 3D inverse opal structures were fabricated with a linear shrinkage of about 1% by means of the selective dissolution of a sintered colloid crystal. In this novel method, the conventional infiltration step that introduces a polymer precursor prior to selective dissolution is not required. Honeycomb or isolated polymer rings can also be produced using this approach, depending on the sintering conditions. The resulting macroporous structures were used in this study as templates for the formation of isolated or interconnected crystalline titania nanorings via the calcination of titanium alkoxide deposited on the templates. The resulting titania nanorings exhibited a robust, undisrupted rutile phase.

Macroporous polymer structures have been a subject of interest in the past few years because of their use in cell cultures,[1] in selective transportation,[2] as catalytic substrates,[3] as insulators,[4] in biomineralization,[5] and as photonic band-gap structures.[6−10] These macroporous structures can also be used as templates for building semiconductor nanoblocks.[11] The inverse opal structure is a macroporous structure that consists of air spheres linked by channels with a high refractive index.[12−16] Although a holographic approach can be utilized in their synthesis,[17] the synthesis of most conventional polymer inverse opals[6−10] proceeds via the infiltration of a polymer precursor into a self-assembled colloidal template. The polymer precursor is then solidified, and the colloidal template is removed by solvent extraction, resulting in the creation of air spheres linked by polymer channels. In this paper, we propose a novel method in which the self-assembled colloids are directly converted to two- or three-dimensional (2D/3D) macroporous structures without the infiltration of a polymer precursor, and we also demonstrate the production of crystalline titania nanorings using these macroporous polymers as templates.

The use of a dual component (soluble/insoluble) colloid system is proposed here as an effective alternative to the conventional template sacrificing method that employs an infiltration step. By selectively dissolving the soluble component of the dual component polymeric colloid crystal, it is possible to produce ordered polymer macroporous structures such as the inverse opal structure. This self-organization approach to the fabrication of inverse opals makes an infiltration step unnecessary. In addition, the resulting macroporous structures can be used as templates for building nanoblocks.[11] Figure 1 shows schematic views of the conventional and novel approaches.

We used monodisperse poly(styrene-*co*-divinylbenzene) (PSDVB) colloids, which consist of cross-linked polydivinylbenzene (PDVB) as the insoluble portion and polystyrene (PS) as the portion soluble in cyclohexane. Supporting Information is available that details the spectroscopic and thermal characterizations of the PSDVB and homo PS colloids that were used in our experiments.

An inverse opal structure composed of PDVB was successfully obtained when a multilayer PSDVB colloid (diameter 500 nm) assembly on a flat epoxy-based azo-functionalized polymer film, hereafter referred to as an azo polymer film, was sintered (125 °C, 1 h) and dissolved in cyclohexane (40 °C, 30 min). The colloidal crystals were formed by convective crystallization, as described previously.[18] Note that the conventional infiltration step was not performed; further information about our procedure is available in Supporting Information. The scanning electron microscopy (SEM) image in Figure 2 of the structure clearly shows interconnected macropores characteristic of inverse opals.

* To whom correspondence should be addressed. E-mail: kimdy@kjist.ac.kr.

10.1021/nl025829l CCC: $25.00
Published on Web 12/17/2002

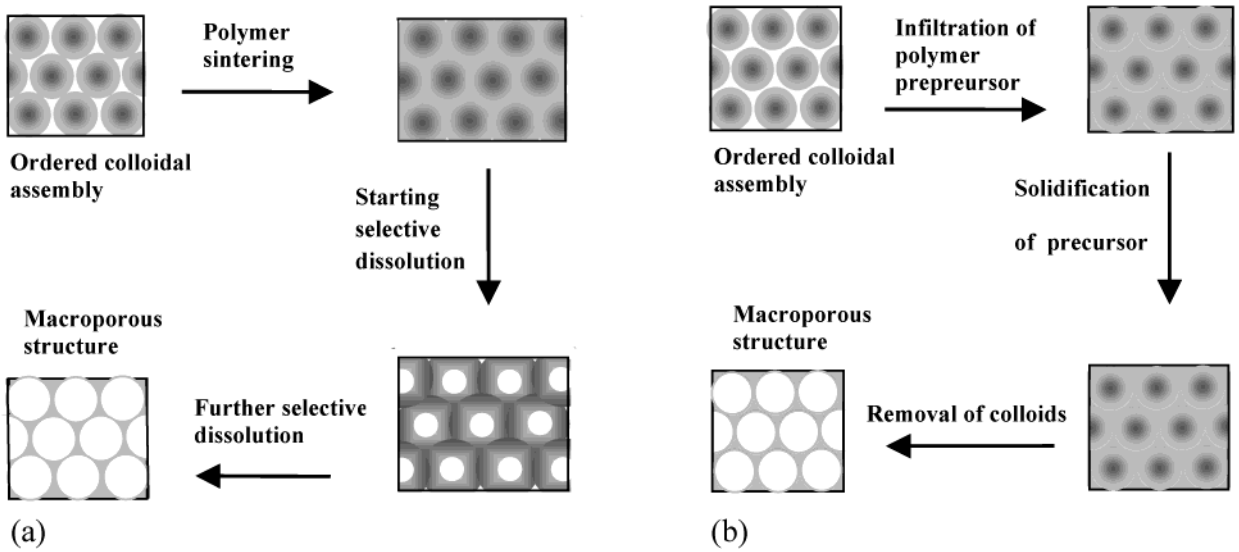

Figure 1. (a) Newly proposed method for the fabrication of macroporous polymer structures. The packing density of the colloid is increased by sintering. Selective dissolution initiates the core opening of the sintered colloid crystal. Further dissolution produces a macroporous structure. No infiltration step was required in the formation of the porous structure. (b) Conventional infiltration method for the fabrication of macroporous polymer structures. The polymer precursor is infiltrated into a self-assembled colloidal template and solidified. The colloidal template structures the polymer precursor, so the template and the resulting channels of the porous structure have different chemistry.

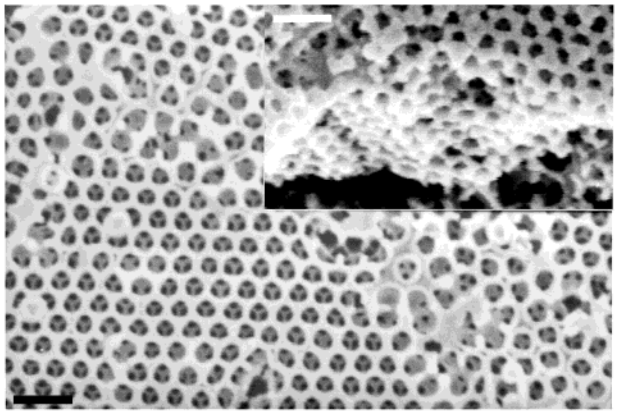

Figure 2. SEM image of an inverse opal is shown with a tripod within a pore. The side view shows that a multilayer inverse opal has been obtained (inset image). Scale bar, 1 μm.

Some openings in the channels were observed (lower right corner of Figure 2). The 3D layer-by-layer development of a macroporous network was confirmed by both a tripod that could be observed within the pore and from the cross section of a fractured sample (inset in Figure 2). The average pore diameter was 348 ± 15 nm, and the average channel width was 162 ± 18 nm. The average center-to-center distance between the pores was 494 ± 8 nm. Since the diameter of the template colloid was 500 nm, the linear shrinkage during the formation of the macroporous network was only about 1%.

This shrinkage is remarkably small in comparison with the shrinkages (5 to 30%) reported for the polymer infiltration method[6−10] or for methods using sol−gel chemistry[19] and indicates that our method is a good approach to the fabrication of polymer inverse opals with high dimensional stability.

To examine the mechanism for the production of the ordered macropores, we arrayed a colloid as a 2D monolayer on a flat azo polymer film; sintering and dissolution with cyclohexane were then carried out. It should be noted that the azo polymer film we used was insoluble in cyclohexane: the azo benzene-functionalized polymers used in our experiments contain polar azo chromophores, so they are insoluble in cyclohexane. No infiltration step was performed. Figure 3 shows SEM images of the resulting structures. The self-assembled 2D monolayer exhibited hexagonal symmetry (Figure 3a). After sintering at 125 °C for 1 h, the formation of hexagonal contacts between the colloid particles was observed (Figure 3b). Then, in the early stages of dissolution (40 °C, 4 min), the formation of a porous structure with channels became evident, and channels near the pores exhibited tumorous pendants (Figure 3c). Further dissolution (30 min) led to the disappearance of the pendants and to the formation of a honeycomb structure (Figure 3d).

The detailed mechanism of the formation of this honeycomb structure is not yet clearly understood. However, our understanding of this process is as follows. During sintering, the contact between the colloid particles increases to lower the total free energy. Mobile PS linear chains intermingle with branched or cross-linked PDVB chains**,** perhaps producing interpenetrating physical cross links at the points of contact, leading to insolubility. As dissolution proceeds, the PDVB chains in the solvent-swollen colloid particles precipitate at the solvent-resistant contacts due to the highly branched or cross-linked nature of the PDVB. This kind of surface coagulation near the PDVB cross-link points has also been reported by Okubo et al.[20] They synthesized a shell of PDVB network onto a PS seed. However, the linear PS chains dissolve and do not remain anchored at the points of contact. Therefore, the extraction process is more active in the centers of the colloid particles, and the contact regions persist as the insoluble channels shown in Figure 3c and d. The magnified image in Figure 3 part e of an area of part d

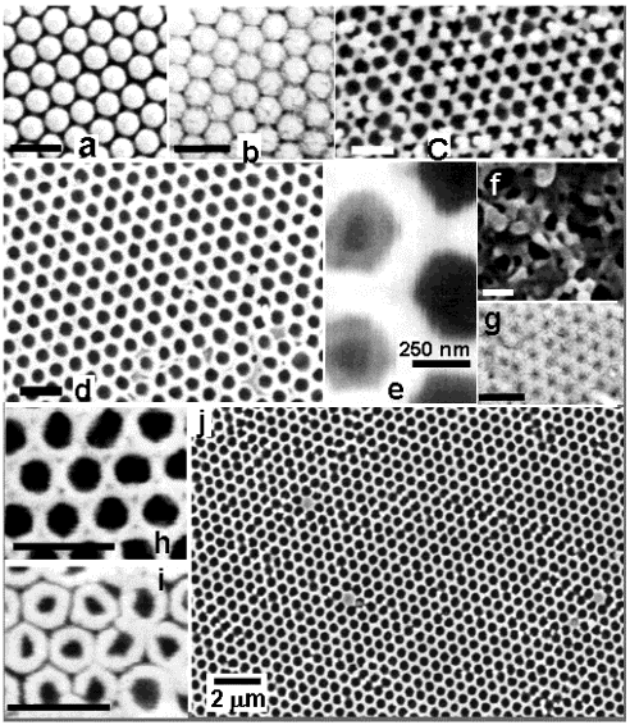

Figure 3. SEM images of (a) a 2D monolayer PSDVB colloid; (b) sintered (at 125 °C) colloid particles; (c) the early stages of dissolution with pendants visible at the particle contacts (4 min); (d) after further dissolution (30 min), a honeycomb structure with no pendants at the contacts; (e) an enlarged view of the local pores of the honeycomb; (f) a monolayer dissolved without sintering; (g) traces on an azo polymer film of an extracted homo PS colloid after dissolution; (h) openings in the channels of the honeycomb; (i) isolated polymer rings in the honeycomb; and (j) a well-organized honeycomb produced by an increase in the sintering temperature to 150 °C. Scale bar (except for panels e and j), 1 μm.

provides supporting evidence for the above discussion. Although most pores show clear openings such as the pores on the right of Figure 3e, the two pores on the left show increasing contrast in a radial direction from the dark centers toward the surrounding contact regions. Since the regions of high contrast correspond to the material remaining after dissolution, it is clear that extraction is more active in the centers of the colloid particles.

To confirm the effects of sintering, we assembled a 2D monolayer as above and without sintering dissolved it in cyclohexane (40 °C, 30 min). The resulting structure was an irregularly linked bush without an ordered honeycomb pattern (Figure 3f). Therefore, it is clear that sintering is required for the formation of ordered, interconnected contacts. It was also shown that the insoluble contacts in the honeycomb consist of PDVB because a sintered homo PS colloid ($T_g \approx 108$ °C, Polysciences catalog number 07307) assembly was found to be totally extracted by cyclohexane in 10 min at 40 °C. However, even in this case, traces of depleted colloid particles[21] were observed as concavities on the azo polymer substrate (Figure 3g). From these considerations, we conclude that both cross linking within the colloid and sintering enable the fabrication of ordered macroporous structures via selective dissolution, without an infiltration step.

The honeycomb structure showed some defects in the form of the small openings in the channels and the isolated polymer rings visible in the lower right corner of Figure 3d. Figure 3h and i show enlarged images of the channel openings and the isolated polymer rings, respectively. The average size of the pores, the average channel width, and the center-to-center distance (between pores) of the honeycomb were 348 ± 10 nm, 171 ± 13 nm, and 497 ± 4 nm, respectively. These values are quite similar to those of the inverse opal described above. However, for the isolated rings, the average pore size and torus width were 213 ± 30 nm and 148 ± 10 nm, respectively. The pore size is tunable on a nanometer or micrometer scale by varying the structure of the template colloid.

Channel openings and ring isolation were not observed when the sintering temperature was increased to 150 °C. This decrease in the number of isolated rings also increased the homogeneity of the honeycomb's hexagonal symmetry (Figure 3j). When the sintering was performed at the lower temperature as described above (Figure 3d, at 125 °C, slightly above T_g), viscous flow[22] was not achieved, so the colloid−colloid interface does not disappear, but soft contact is made between the colloid particles. This mild sintering produces channel openings and ring isolation during dissolution. We employed these openings and the isolated polymer rings to produce isolated TiO_2 rings, as described below.

We extended our experiment to the fabrication of novel building blocks, crystalline titania nanorings. Although numerous types of nanoblocks have been studied,[23] semiconductor nanoblocks are of particular interest because of their novel optical and electronic properties. However, there is still a limited understanding of crystalline semiconductor rings.

A honeycomb and an inverse opal were used as templates for fabricating the nanorings. When the TiO_2 precursor was spun onto a honeycomb-type template (sintered at 125 °C) and calcined at 900 °C, both interconnected (sharing a torus) (Figure 4a) and isolated rings were produced (Figure 4b). Titanium isopropoxide was selectively adsorbed onto the channels because of the π-donating ligand properties of phenyl groups[11] but was not adsorbed in the air spheres, and titania rings were produced during calcination. A free-standing film containing titania rings can be made by peeling the titanium isopropoxide deposited film away from the quartz plate before calcination. The average pore diameter of the interconnected rings decreased to 257 ± 35 nm (∼348 nm in the template) and the average channel width increased to 242 ± 23 nm (∼171 nm in the template) because of the adsorption of titanium isopropoxide onto the inner surface of the pores. However, the center-to-center distance between the pores remained relatively constant (∼492 ± 9 nm, as for the template). The sizes of the tori (152 ± 16 nm) and the pores (211 ± 83 nm) of isolated rings were relatively unchanged in comparison to those of the template, but the irregularity of the pores increased. A depth profile (Figure 4c) was obtained using AFM through the three rings indi-

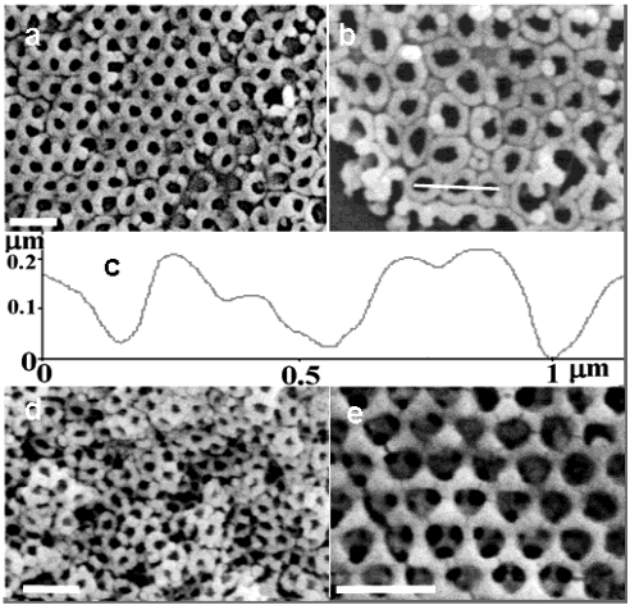

Figure 4. SEM images of (a) 2D interconnected and (b) isolated titania rings fabricated on the honeycomb template. (c) AFM depth profile of the three rings indicated by the line at the bottom of (b). (d) 3D pile of titania rings created by using an inverse opal template and calcination of the deposited titanium alkoxide at 900 °C. (e) As-deposited (before calcination) structure, showing an inverse opal order. Scale bar, 1 μm.

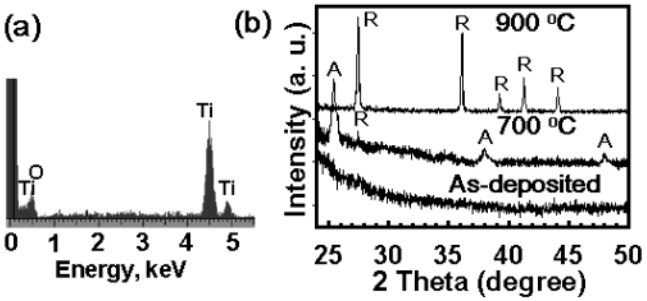

Figure 5. (a) EDX spectra showing that the titania rings are composed of Ti and O. (b) XRD data indicating that the crystalline phase of the interconnected titania rings is a mixture of anatase and rutile (calcined at 700 °C) or whole rutile (calcined at 900 °C). A: anatase, R: rutile.

cated by the line in Figure 4b. It is clear that neighboring rings do not share tori but have their own tori (thickness 120−200 nm).

A 3D pile of chain rings, including locally isolated rings, was obtained by using the inverse opal as a template (Figure 4d). Although the as-deposited material maintained an inverse opal order (Figure 4e), this order was disrupted by calcination at 900 °C. Such disordering at high temperatures is well known, but no destruction of macropores was evident; the pore diameter (188 ± 14 nm) was significantly less than that of the 2D interconnected rings. Energy-dispersive X-ray spectroscopy (EDX) of the 2D and 3D titania rings reveals that the rings consist of TiO_2 (Figure 5a). X-ray diffraction (XRD) patterns before and after calcination of a titanium isopropoxide-deposited inverse opal showed that the crystalline phase was converted from an amorphous phase (as-deposited) to a mixture of anatase and rutile (700 °C) or to whole rutile (900 °C) by increasing the calcination temperature (Figure 5b).

The resulting 2D and 3D titania ring assemblies can be used as photocatalysts, and the feasibility of their fabrication on a conducting glass extends the potential of these assemblies as gas sensors[24] or as photo-/electrochromic materials. Recently, great interest has been shown in the 3D macroporous rutile phase of titania because of its photonic band properties.[25] Although in the present study ring shape was maintained and a 3D titania ring assembly was obtained in the rutile phase, the formation of rutile 3D porous structures with long-range order remains a challenge. However, from a photonics viewpoint, this structure may not be particularly desirable since it would not produce a full band gap.

The present study demonstrates a novel method for fabricating 2D and 3D polymer macroporous structures and their application as templates for the production of crystalline titania nanorings. Selective dissolution of a sintered colloid assembly permitted the fabrication of 2D honeycomb and 3D polymer inverse opal structures without the use of an infiltration step. The low level of shrinkage (∼1%) and the possibility of pore tunability serve to extend the method's applicability. In addition, the polymer templates served as good adsorption sites for titania precursors for the fabrication of isolated or interconnected TiO_2 nanorings. Robust titania rings were formed in the rutile phase without any detectable disruption, even at 900 °C.

Acknowledgment. This work was supported by the NRL program KOSEF (R01-2001-00324) and by the Korea Energy Management Corporation.

Supporting Information Available: Detailed explanation of procedures. This material is available free of charge via the Internet at http://pubs.acs.org.

References

(1) Nishikawa, T.; Nishida, J.; Ookura, R.; Nishimura, S. I.; Wada, S.; Karino, T.; Shimomura, M. *Mater. Sci. Eng., C* **1999**, *8*−*9*, 495.
(2) Yoshida, M.; Asano, M.; Safranj, A.; Omichi, H.; Spohr, R.; Vetter, J.; Katakai, R. *Macromolecules* **1996**, *29*, 8987.
(3) Tanev, P. T.; Chibwe, M.; Pinnavaia, T. J. *Nature (London)* **1994**, *368*, 321.
(4) Senkevich, J. J.; Desu, S. B. *Appl. Phys. Lett.* **1998**, *72*, 258.
(5) Meldrum, F. C. *Nanoparticles and Nanostructured Films*; Wiley-VCH: Weinheim, Germany, 1998.
(6) Wang, D.; Caruso, F. *Adv. Mater.* **2001**, *13*, 350.
(7) Miguez, H.; Meseguer, F.; Lopez, C.; Lopez-Tejeira, F.; Sanchez-Dehesa, J. *Adv. Mater.* **2001**, *13*, 393.
(8) Deutsch, M.; Vlasov, Y. A.; Norris, D. J. *Adv. Mater.* **2000**, *12*, 1176.
(9) Gates, B.; Yin, Y.; Xia, Y. *Chem. Mater.* **1999**, *11*, 2827.
(10) Jiang, P.; Hwang, K. S.; Mittleman, D. M.; Bertone, J. F.; Colvin, V. L. *J. Am. Chem. Soc.* **1999**, *121*, 11630.
(11) Jiang, P.; Bertone, J. F.; Colvin, V. L. *Science (Washington, D.C.)* **2001**, *291*, 453. Jiang et al. suggested that polymer inverse opal could be a good template for fabricating solid or hollow TiO_2 spheres.
(12) Reference 11, an example of a TiO_2 channel.
(13) Example of a silicon channel: Blanco, A.; Chomski, E.; Grabtchak, S.; Ibisate, M.; John, S.; Leonard, S. W.; Meseguer, F.; Miguez, H.; Mondia, J. P.; Ozin, G. A.; Toader, O.; Van Driel, H. M. *Nature (London)* **2000**, *405*, 437.
(14) Examples of a CdSe channel: Vlasov, Y. A.; Yao, N.; Norris, D. J. *Adv. Mater.* **1999**, *11*, 165. Davidoff, J.; Davies, I.; Roberson, D. *Nature (London)* **1999**, *402*, 603.

(15) Example of a Au channel: Velev, O. D.; Tessier, P. M.; Lenhoff, A. M.; Kaler, E. W. *Nature (London)* **1999**, *401*, 548.
(16) Example of a Ag channel: Lellig, C.; Hartl, W.; Wagner, J.; Hempelmann, R. *Angew. Chem., Int. Ed*. **2002**, *41*, 102.
(17) Campbell, M.; Sharp, D. N.; Harrison, M. T.; Denning, R. G.; Turberfield, A. J. *Nature (London)* **2000**, *404*, 53.
(18) Kralchevsky, P. A.; Nagayama, K. *Langmuir* **1994**, *10*, 23. Dekov, N. D.; Velev, O. D.; Kralchevsky, P. A.; Ivanov, I. B.; Yoshimura, H.; Nagayama, K. *Langmuir* **1992**, *8*, 3183. Yi, D. K.; Kim, M. J.; Kim, D. Y. *Langmuir* **2002**, *18*, 2019.
(19) Wijnhoven, J. E. G. J.; Vos, W. L. *Science (Washington, D.C.)* **1998**, *281*, 802. Holland, B. T.; Blanford, C. F.; Stein, A. *Science (Washington, D.C.)* **1998**, *281*, 538.
(20) Okubo, M.; Minami, H. *Colloid Polym. Sci.* **1997**, *275*, 992.
(21) Yi, D. K.; Seo, E. M.; Kim, D. Y. *Appl. Phys. Lett.* **2002**, *80*, 225. Lin, K.; Crocker, J. C.; Prasad, V.; Schofield, A.; Weitz, D. A.; Lubensky, T. C.; Yodh, A. G. *Phys. Rev. Lett*. **2000**, *85*, 1770. Yi, D. K.; Seo, E. M.; Kim, D. Y. *Langmuir* **2002**, *18*, 5321.
(22) Frenkel, J. *J. Phys.* **1945**, *9*, 385. Kuczynski, G. C. *J. Appl. Phys.* **1949**, *20*, 1160.
(23) (a) Hollow nanosphere: Caruso, F.; Caruso, R. A.; Mohbald, H. *Science (Washington, D.C.)* **1998**, *282*, 1111. Zhong, Z.; Yin, Y.; Gates, B.; Xia, Y. *Adv. Mater*. **2000**, *12*, 206. (b) Tubules and fibrils: Lakshmi, B. B.; Dorhout, P. K.; Martin, C. R. *Chem. Mater*. **1997**, *9*, 857. (c) Wire form: Wu, Y.; Yang, P. *J. Am. Chem. Soc.* **2001**, *123*, 3165. Martin, C. R. *Science (Washington, D.C.)* **1994**, *266*, 1961. Cheng, G. S.; Zhang, L. D.; Zhu, Y.; Fei, G. T.; Li, L.; Mo, C. M.; Mao, Y. Q. *Appl. Phys. Lett.* **1999,** *75*, 2455. Yi, D. K.; Yoo, S. J.; Kim, D. Y. *Nano Lett.* **2002**, *2*, 1101. Huber, C. A.; Huber, T. E.; Sadoqi, M.; Lubin, J. A.; Manalis, S.; Prater, C. B. *Science (Washington, D.C.)* **1994**, *263*, 800. Nielsch, K.; Muller, F.; Li, A.; Gosele, U. *Adv. Mater*. **2000**, *12*, 582. Chen, G. S.; Boothroyd, C. B.; Humphreys, C. J. *Appl. Phys. Lett.* **1993**, *62*, 1949. Liu, H. I.; Biegelsen, D. K.; Ponce, F. A.; Johnson, N. M.; Pease, R. F. W. *Appl. Phys. Lett.* **1994,** *64*, 1383. (d) Nanoribbons: Shi, W.; Peng, H.; Wang, N.; Li, C. P.; Xu, L.; Lee, C. S.; Kalish, R.; Lee, S.-T. *J. Am. Chem. Soc.* **2001**, *123*, 11095. (e) Nanorods: Hu, J.; Li, L.; Yang, W.; Manna, L.; Wang, L.; Alivisatos, A. P. *Science (Washington, D.C.)* **2001**, *292*, 2060. Puntes, V. F.; Krishnan, K. M.; Alivisatos, A. P. *Science (Washington, D.C.)* **2001**, *291*, 2115. (f) Vesicle sphere: Lu, Y.; Fan, H.; Stump, A.; Ward, T. L.; Rieker, T.; Brinker, C. J. *Nature (London)* **1999**, *398*, 223.
(24) Savage, N.; Chwieroth, B.; Ginwalla, A.; Patton, B. R.; Akbar, S. A.; Dutta, P. K. *Sens. Actuators, B* **2001**, *79*, 17, using the mixture of rutile (as a p-type semiconductor) and anatase (as an n-type semiconductor).
(25) Subramanian, G.; Manoharan, V. N.; Thorne, J. D.; Pine, D. J. *Adv. Mater.* **1999**, *11*, 1261.

NL025829L